Macromolecules

ARTICLE

pubs.acs.org/Macromolecules

Formation Kinetics and Scaling of "Defect-Free" Hyperbranched Polystyrene Chains with Uniform Subchains Prepared from Seesaw-Type Macromonomers

Lianwei Li,[†] Chen He,[‡] Weidong He,*[,‡] and Chi Wu*[,†,§]

[†]Hefei National Laboratory for Physical Sciences at Microscale, Department of Chemical Physics, University of Science and Technology of China, Hefei, China 230026

[‡]CAS Key Laboratory of Soft Matter Chemistry, Department of Polymer Science and Engineering, University of Science and Technology of China, Hefei, China 230026

[§]Department of Chemistry, The Chinese University of Hong Kong, Shatin N. T., Hong Kong

ABSTRACT: Using a facile approach, we successfully made large "defect-free" hyperbranched polystyrene (PSt) chains with uniform subchains between two branching points from the interchain "clicking" of a seesaw-type linear macromonomer [azide∼∼∼alkyne∼∼∼azide] prepared by ATRP with a following conversion of two bromine-ends into two azide-ends, where ∼∼∼ denotes a PSt chain (1.65−31.0 kg/mol). The "click" reaction kinetics monitored by a combination of size exclusion chromatography (SEC) and laser light scattering (LLS) reveals that the degree of self-polycondensation (DP) is related to the reaction time (t) as $\ln(\mathrm{DP}+1)/2 = ([\mathrm{A}]_0 k_{AB,0})/\beta \arctan(\beta t)$, where $[\mathrm{A}]_0$ and $k_{AB,0}$ are the initial alkyne concentration and the initial reaction rate between the azide and alkyne groups, respectively; β is a constant and its reciprocal ($1/\beta$) represents the time at which $k_{AB} = k_{AB,0}/2$. The results reveal that $1/\beta$ is scaled to the macromonomer's molar concentration ($[\mathrm{C}]$) and molar mass (M) as $1/\beta \sim [\mathrm{C}]^{-0.35} M^{0.55}$, indicating that $1/\beta$ is governed by the interchain distance and diffusion, respectively. Each hyperbranched sample can be further fractionated into a set of narrowly distributed "defect-free" hyperbranched chains with different molar masses by precipitation. The LLS results show, *for the first time*, that the root-mean-square radius of gyration ($\langle R_g \rangle$) and hydrodynamic radius ($\langle R_h \rangle$) of "defect-free" hyperbranched polystyrenes in toluene at 25 °C are scaled to the weight-average molar mass (M_w) as $\langle R_g \rangle = 5.53 \times 10^{-2} M_w^{0.464}$ and $\langle R_h \rangle = 2.95 \times 10^{-2} M_w^{0.489}$, respectively, where the exponents are smaller than the predicted $^1/_2$.

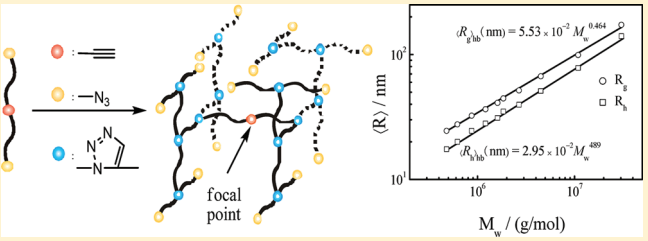

INTRODUCTION

Hyperbranched polymers have unique properties in solution, melt and bulk because of their branched and relatively compact structure in comparison with linear counterparts. Therefore, they have received much attention in the last few decades due to some potential applications in biomedicines, energy storages and polymer blends, to name but a few.[1−5] It has been known that their molecular parameters, such as monomer nature, overall molar mass, polydispersity, branching degree, and distribution of subchain lengths, strongly affect their final macroscopic properties. In order to establish a structure−property relationship, a set of narrowly distributed hyperbranched samples (standards) with a well-defined structure and uniform subchains but different overall molar masses have to be prepared before any possible study. Previously, great efforts have been spent in synthesizing well-defined cyclic,[6−8] star branched,[9,10] mikto-star,[11,12] and H-shaped[13] polymers. Some of their structure−property relationships have been revealed. However, the preparation and study of "defect-free" hyperbranched polymers with uniform and long subchains is rather difficult if not impossible, which hinders the study of their structure−property relationships.[14,15]

As expected, hyperbranched polymers with long subchains between two neighboring branching points are easier to form interchain entanglements in semi/concentrated solutions as well as in bulk, resulting in much tougher polymer materials with an excellent mechanical property. Up to now, hyperbranched polymers can be prepared by self-condensing vinyl or ring-opening polymerization (SCVP[16−19] and SCROP[20,21]) or more used polycondensation.[22−28] The SCVP initially reported by Fréchet et al.[19] is fairly versatile, in which hyperbranched chains are formed via polymerization of vinyl macromonomers with an initiating group. While in SCROP, a polymerizable cyclic group is used instead of a vinyl group. However, SCVP and SCROP have their own disadvantages. For example, side reactions could lead to the formation of a gel and a broad distribution of the subchain length.[29] Note that an ideal hyperbranched chain should have an identical number of strands that are connected onto each

Received: July 22, 2011
Revised: September 6, 2011
Published: September 28, 2011

Scheme 1. Comparison of Topological Structures of a Randomly Branched Chain and a Hyperbranched Chain Prepared by Using Different Types of Macromonomers

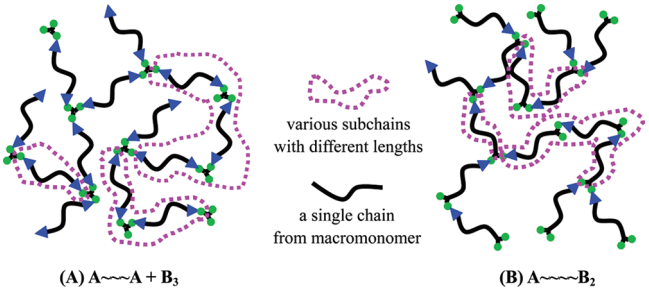

branching point, resulting in uniform subchains between two neighboring branching points.[30,31]

Scheme 1 shows two typical approaches in the preparation of hyperbranched chains: (A) polycondensation[32−34] and (B) self-polycondensation.[3,14,15,35−38] The polycondensation between A_2 and B_3 is one of the earliest adopted synthetic strategies. For example, Unal et al.[32] used an A_2-type isocyanate end-capped propylene oxide or tetramethylene oxide oligomers and a B_3-type triamine branching agent to make randomly branched polyureas and poly(urethane urea)s. Similarly, hyperbranched poly(esterurethane)s (HB-PEU) was prepared with a B_3-type trifunctional ε-caprolactone oligomers and an A_2-type isocyanated 1,4-butanediol monomer.[33] On the other hand, the self-polycondensation of Y-type macromonomers ($A\sim\sim\sim\sim B_2$) were extensively used to prepare hyperbranched polymers with long subchains. Hedrick et al.[34] prepared hyperbranched poly(ε-caprolactone)s (HPCL) using short PCL chains with one carboxylic acid end and two hydroxyl groups at the other chain end. Bo et al.[27] started with a short chain with one boronic ester at one end and two bromo functional groups at the other end to synthesize hyperbranched chains via the Suzuki reaction. Hutchings et al.[14,15,35,36] prepared hyperbranched polystyrene (PSt) made of a trifunctional macromonomer with one chloride at one end and two phenol groups at the other end via the Williamson reaction and studied their theology properties. Pan et al.[37] synthesized hyperbranched PSt chains made of a macromonomer with two alkyne groups at one end and one azide group at the other end using the "click" reaction. Konkolewicz et al.[38] prepared hyperbranched PSt chains using the thiol−yne "click" trick, where one end contains a thiol group and the other end contains a alkyne groups. As shown in Scheme 1, these two mostly used approaches unavoidably result in subchains with different lengths because of some unreacted B-groups; namely, each unreacted B group extends the subchain by one macromonomer length.

Recently, we adopt a slightly different approach. Instead of putting two reactive B groups on one end, we attach them, respectively, at two ends of our macromonomer and move the reactive A group to the middle, i.e., a seesaw-type $B\sim\sim\sim\sim A\sim\sim\sim\sim B$ chain, as schematically shown in Scheme 2. In this way, each resultant hyperbranched chain, no matter how large it is, contains no more than one unreacted A group if it does no undergo an intrachain cyclization with one of B groups inside. Otherwise, the cyclization will lead to a loop, the only possible "defect" inside the entire hyperbranched chain. During the self-polycondensation, macromonomers continuously react and add to the branched chain, finally leading to large hyperbranched chains with uniform subchains; namely, each subchain is exactly made of half a macromonomer. For such formed large hyperbranched chains, one possible "defect" (self-looping) has nearly no effect on their properties. This is why we still name them as "defect-free". It should be emphasized that such formed chains are different from dendrimers. Hedrick et al.[39] and Kwak et al.[40] previously used this approach to synthesize hyperbranched chains, starting with short B∼A∼B oligomers containing 5−20 monomer units. Their resultant hyperbranched polymers are too small to be accurately characterized by laser light scattering (LLS), presumably because they used a relatively lower efficient esterification.

To the best of our knowledge, no one has tried to use this kind of linear seesaw-type long $B\sim\sim\sim\sim A\sim\sim\sim\sim B$ chains to prepare large hyperbranched polymers with long and uniform subchains and seriously study their formation kinetics and scaling laws between their size and overall mass. Recently, we first studied how the macromonomer length and concentration affect the cyclization of linear seesaw-type macromonomers and their influence on resultant hyperbranched chains.[41] In the current study, using similar linear B∼∼PSt∼∼A∼∼PSt∼∼B macromonomers with different lengths, we were able to prepare and characterize a series of large hyperbranched polystyrenes with uniform subchains by a combination of the activators regenerated by electron transfer for atom transfer radical polymerization (ARGET ATRP) and "click" chemistry. The self-polycondensation kinetics was monitored by a combination of size exclusion chromatography (SEC) and LLS. We purposely varied the subchain length from shorter to twice longer than the entanglement length ($M_e \sim 1.8 \times 10^4$ g/mol for polystyrene). The fractionation of each resultant broadly distributed hyperbranched polystyrene sample by precipitation led to a set of "defect-free" narrowly distributed hyperbranched polystyrene chains with uniform subchains but different overall molar masses. We have, *for the first time*, experimentally elucidated their formation kinetics and established scaling laws between their size and overall mass. Armed with such prepared hyperbranched chains, we will be able to further study correlations between their microscopic structures and macroscopic properties.

EXPERIMENTAL SECTION

Materials. Styrene (St, Sinopharm, 97%) was first passed through a basic alumina column to remove inhibitor and then distilled under reduced pressure over CaH_2. Dimethylformamide (DMF, Sinopharm, AR) was first dried with anhydrous magnesium sulfate and then distilled under reduced pressure prior to use. Dichloromethane (DCM) and triethylamine (TEA) from Sinopharm were distilled over CaH_2 just prior to use. Tris(2-(dimethylamino)ethyl)amine (Me_6TREN) was synthesized by following a procedure described in literature.[42] Copper(I) bromide (CuBr, Alfa, 98%) was washed with glacial acetic acid to remove soluble oxidized species, filtrated, washed with ethanol and dried under vacuum. *N*,*N*,*N*′,*N*′,*N*″-Pentamethyldiethylenetriamine (PMDETA, Aldrich, 99%), anisole (Alfa, 99%), 2,2′-bipyridine (bpy, Fluka, 99%), sodium azide (NaN_3, Aldrich, 99%), 2,2-bis(hydroxymethyl) propionic acid (DMPA, Fluka, 97%), *N*,*N*-dimethyl-4-amidopyridine (DMAP, Aladdin, 99%), dicyclohexyl carbodiimide (DCC, Aladdin, 99%), 2-bromoisobutyryl bromide (Aladdin, 98%), *p*-toluenesulfonic acid monohydrate (PTSA, Aladdin, 99%), 2,2-dimethoxypropane (DMP, Aladdin, 99%), propargyl alcohol (Aldrich, 99%), and tin(II)-2-ethylhexanoate ($Sn(EH)_2$, Aladdin, 95%) and other analytic grade reagents from Sinopharm were used as received.

Scheme 2. Schematic Synthesis of Macromonomer and Hyperbranched Polystyrene

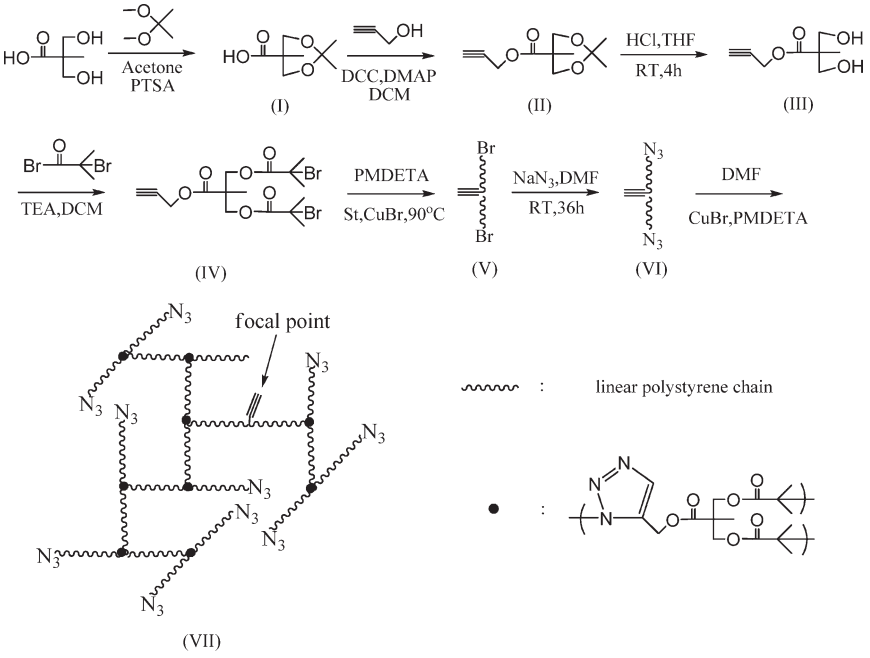

Size Exclusion Chromatography. The relative number- and weight-average molar masses ($M_{n,SEC}$ and $M_{w,SEC}$) and the absolute number- and weight-average molar masses ($M_{w.MALLS}$ and $M_{w,MALLS}$) were determined at 35 °C by size exclusion chromatography (SEC, Waters 1515) equipped with three Waters Styragel columns (HR2, HR4, HR6), respectively, equipped with a refractive index (RI, Wyatt WREX-02, using a conventional universal calibration with linear polystyrene standards) detector and a multiangle LLS (MALLS, Wyatt DAWN EOS) detector. Note that SEC measures the weight distribution of hyperbranched chains ($W(M)$ or $C(M)$. The values of M_n and M_w are calculated, respectively, using

$$M_{n,MALLS} = \frac{\sum C_i}{\sum C_i/M_i}, \quad M_{w,MALLS} = \frac{\sum C_i M_i}{\sum C_i} \tag{1}$$

THF was used as an eluenting agent at a flow rate of 1.0 mL/min. The MALLS detector uses a GaAs laser (685 nm and 30 mW) and has 18 diodes placed at different angles, ranging from 22.5 to 147.0°. The data were analyzed using ASTRA for Windows software (Ver. 4.90.07, Wyatt). The dn/dC of polystyrene in THF was 0.185 mL/g at 30 °C. For both SEC-RI and SEC-MALLS measurements, 1 mL of polymer solution (2−8 mg/mL, depending on the molar mass) was prefiltered through a 0.2-μm PVDF filter before injection.

Laser Light Scattering. A commercial LLS spectrometer (ALV/DLS/SLS-5022F) equipped with a multi-τ digital time correlator (ALV5000) and a cylindrical 22 mW UNIPHASE He−Ne laser (λ_0 = 632.8 nm) as the light source was used. In static LLS,[43,44] the angular dependence of the absolute excess time-average scattering intensity, known as the Rayleigh ratio $R_{VV}(q)$, can lead to the weight-average molar mass (M_w), the root-mean-square gyration radius $\langle R_g^2\rangle_Z^{1/2}$ (or simply written as $\langle R_g\rangle$) and the second virial coefficient A_2 by using

$$\frac{KC}{R_{VV}(q)} \cong \frac{1}{M_w}\left(1 + \frac{1}{3}\langle R_g^2\rangle_Z q^2\right) + 2A_2C \tag{2}$$

where $K = 4\pi^2(\mathrm{d}n/\mathrm{d}C)^2/(N_A\lambda_0^4)$ and $q = (4\pi/\lambda_0)\sin(\theta/2)$ with C, dn/dC, N_A, and λ_0 being concentration of the polymer solution, the specific refractive index increment, Avogadro's number, and the wavelength of light in a vacuum, respectively. The extrapolation of $R_{VV}(q)$ to $q \to 0$ and $C \to 0$ leads to M_w. The plot of $[KC/R_{VV}(q)]_{C\to 0}$ vs q^2 and $[KC/R_{VV}(q)]_{q\to 0}$ vs C lead to $\langle R_g^2\rangle_Z$ and A_2, respectively. In a very dilute solution, the term of $2A_2C$ can be ignored. For relatively small scattering objects, the Zimm plot on the basis of eq 2 incorporates the extrapolations of $q \to 0$ and $C \to 0$ on a single grid. For long polymer chains, i.e., $q\langle R_g\rangle > 1$, the Berry plot is normally used. In static LLS, the scattering intensity was recorded at each angle three times and each time was averaged over 30 s. The scattering angle ranges from 12 to 120°. The refractive index increment of hyperbranched polystyrenes in toluene (dn/dC = 0.111 mL/g at 25 °C and 633 nm) was determined by a precise differential refractometer.[45]

In dynamic LLS,[46] the Laplace inversion of each measured intensity−intensity time correlation function $G^{(2)}(q,t)$ in the self-beating mode can lead to a line-width distribution $G(\Gamma)$, where q is the scattering vector. For dilute solutions, Γ is related to the translational diffusion coefficient D by $(\Gamma/q^2)_{q\to 0,C\to 0} \to D$, so that $G(\Gamma)$ can be converted into a transitional diffusion coefficient distribution $G(D)$ or further a hydrodynamic radius distribution $f(R_h)$ via the Stokes−Einstein equation, $R_h = (k_BT/6\pi\eta_0)/D$, where k_B, T and η_0 are the Boltzmann constant, the absolute temperature and the solvent viscosity, respectively. The polydispersity index M_w/M_n was estimated from $M_w/M_n \approx (1 + 4\mu_2/\langle D\rangle^2)$, where $\mu_2 = \int_0^\infty G(D)(D - \langle D\rangle)^2 \mathrm{d}D$. In dynamic LLS experiments, we used a fixed small angle (12°) to ensure that the effect of extrapolating to the zero angle is minimum. The time correlation functions were analyzed by both the cumulants and CONTIN analysis.

Chemical Synthesis. Scheme 2 shows a schematic chemical synthesis of different chemicals required to prepare linear seesaw-type macromonomer chains with two azide end groups and one middle alkyne group as well as the self-polycondensation via "click" chemistry between azide and alkyne.

Isopropylidene-2,2-bis(methoxy)propionic Acid (***I***). 2,2-Bis(hydroxymethyl)propionic acid 30.00 g (223.7 mmol), 2,2-dimethoxypropane (41.4 mL, 335.4 mmol), and *p*-toluenesulfonic acid monohydrate (2.10 g, 11.1 mmol) were dissolved in 100 mL of acetone. The mixture was stirred for 4 h at room temperature before 3.0 mL of a mixture of an ammonia solution (25%) and EtOH (50/50, v/v)) was added into the reaction

dx.doi.org/10.1021/ma201687s |*Macromolecules* 2011, 44, 8195–8206

mixture to neutralize the catalyst. The solvent was removed by evaporation under reduced pressure at room temperature. The residue was then dissolved in CH_2Cl_2 (600 mL) and extracted with two portions of water (80 mL). The organic phase was dried with anhydrous Na_2SO_4 and evaporated to give **I** as white powder (33.0 g, 84%). The ^{1}H NMR spectra were recorded on a commercial Bruker AV400 NMR spectrometer using $CDCl_3$ as solvent and tetramethylsilane (TMS) as an internal standard. ^{1}H NMR ($CDCl_3$, ppm): δ 4.18 (d, 2H, $-CH_2O(CH_3)C(CH_3)OCH_2-$), 3.65 (d, 2H, $-CH_2O(CH_3)C-(CH_3)OCH_2-$), 1.41(s, 3H, $-CH_2O-(CH_3)C(CH_3)OCH_2-$), 1.38 (s, 3H, $-CH_2O(CH_3)C(CH_3)-OCH_2-$), 1.20 (s, 3H, $CH_3C(CH_2O-)_2COOH$).

*Propargyl 2,2,5-Trimethyl-1,3-dioxane-5-carboxylate (**II**).* Propargyl alcohol (14.7 mL, 256 mmol), isopropylidene-2,2-bis(methoxy)-propionic acid (**I**) (29.8 g, 172 mmol), and DMAP (10.2 g, 84 mmol) was dissolved in 300 mL CH_2Cl_2. After stirring at room temperature for 10 min, DCC (42 g, 204 mmol) dissolved in 100 mL of CH_2Cl_2 was added dropwise into the mixture within 30 min under N_2 flow. Reaction mixture was stirred overnight at room temperature and urea byproduct was filtrated. The solution was then diluted by CH_2Cl_2 (800 mL) and extracted with two portions of water (150 mL), and the organic phase was dried with anhydrous Na_2SO_4. The solvent was evaporated, and the remaining product was purified by column chromatography over silica gel eluting with hexane/ethyl acetate (25:1, v/v) to give a colorless clear oil: 25.0 g (69%). ^{1}H NMR ($CDCl_3$, ppm): δ 4.74 (d, 2H, $CH{\equiv}CCH_2O-$), 4.20 (d, 2H, $-CH_2O(CH_3)C(CH_3)OCH_2-$), 3.67 (d, 2H, $-CH_2O(CH_3)C(CH_3)OCH_2$-), 2.48 (t, 1H, $CH{\equiv}CCH_2O-$), 1.43 (s, 3H, $-CH_2O(CH_3)C(CH_3)OCH_2-$), 1.39 (s, 3H, $-CH_2O-(CH_3)C(CH_3)O-CH_2-$), 1.22 (s, 3H, $CH_3C(CH_2O-)_2COOH$).

*Propargyl 3-Hydroxy-2-(hydroxymethyl)-2-methylpropanoate (**III**).* Propargyl 2,2,5-trimethyl-1,3-dioxane-5-carboxylate (II) (10.0 g, 47.5 mmol) was dissolved in a mixture of 1 M HCl (25 mL) and THF (25 mL). The reaction mixture was stirred for 4 h at room temperature. The precipitated product was filtrated off, and reaction mixture was then diluted by CH_2Cl_2 (400 mL) and extracted with two portions of water (70 mL) and the organic phase was dried with anhydrous Na_2SO_4 and concentrated. Hexane was added to the reaction mixture, and it was kept in deep freeze for 48 h to give white solid: 7.0 g (90%). ^{1}H NMR ($CDCl_3$, ppm): 4.77 (d, 2H, $CH{\equiv}CCH_2O-$), 3.93 (d, 2H, $-CH_2OH$), 3.74 (d, 2H, $-CH_2OH$), 2.73 (br, 2H, -OH), 2.50 (t, 1H, $CH{\equiv}CCH_2O-$), 1.10 (s, 3H, $-CH_3$).

*Propargyl 2,2-Bis((2′-bromo-2′-methylpropanoyloxy)methyl)propionate (**IV**).* Propargyl 3-hydroxy-2-(hydroxymethyl)-2-methylpropanoate (**III**) (4.5 g, 26.0 mmol) was first dissolved in 90 mL of CH_2Cl_2, and then triethyl amine (8.0 mL, 57.5 mmol) was added. After the mixture was cooled to 0 °C, 2-bromoisobutryl bromide (6.05 g, 26.0 mmol) in 40 mL of CH_2Cl_2 was added dropwise within 30 min. The reaction mixture was stirred overnight. After filtration, the mixture was extracted with CH_2Cl_2 (200 mL) and saturated aq. $NaHCO_3$ (50 mL). The aqueous phase was again extracted with CH_2Cl_2 (100 mL) and the combined organic phase was dried with anhydrous Na_2SO_4. The solution was concentrated and the crude product was purified by column chromatography over silica gel eluting with hexane/ethyl acetate (4:1, v/v) to give white crystal: 7.1 g (87%). ^{1}H NMR ($CDCl_3$, ppm): δ 4.74 (d, 2H, $CH{\equiv}CCH_2O-$), 4.37 (m, 4H, $-COOCH_2-$), 2.47 (t, 1H, $CH{\equiv}CCH_2O-$), 1.92 (s, 12H, $-CBr(CH_3)_2$), 1.37 (s, 3H, $-CH_3$).

*Polystyrene [alkyne-(PSt-bromine)$_2$] (**V**) via an ARGET ATRP.* The general procedure was as follows. A three-necked flask equipped with a magnetic stirring bar and three rubber septum was charged with PBMP (0.1 g, 0.210 mmol), St (24 mL, 210.0 mmol), Me_6TREN (55.4 μL, 0.210 mmol), $Sn(EH)_2$ (68.0 μL, 0.210 mmol) and anisole (24 mL). The flask was degassed by four freeze−pump−thaw cycles, and then placed in an oil bath thermostated at 90 °C. After ~2 min, CuBr (3 mg, 0.021 mmol) was introduced to start the polymerization under N_2 flow. After a few hours, the flask was rapidly cooled to room temperature and quenched with $CuBr_2$. The polymer mixture was diluted with THF, and passed through a short column of neutral alumina for the removal of metal salt. After removing all the solvents by a rotary evaporator, the residue was dissolved in THF and precipitated into an excess of methanol. The above purification cycle was repeated twice. After drying in a vacuum oven overnight at room temperature, polystyrene [alkyne-(PSt-bromine)$_2$] (**V**) was obtained (Table 1, entry 14). Yield: 8.1 g (37%). M_n: 4.50 × 10^4 g/mol. M_w/M_n: 1.13 (by SEC).

Table 1. Characterization of Linear PSt Chains Prepared by Normal and ARGET ATRP

		molar ratios						
entry[a,b]	ligand	PBMP	St	CuBr	ligand	$Sn(EH)_2$	M_n,[c] g/mol	M_w/M_n[c]
1	bpy	1	500	2	4	0	1.32×10^4	1.22
2	bpy	1	1000	2	4	0	2.33×10^4	1.25
3	bpy	1	1000	2	4	0	2.71×10^4	1.27
4	bpy	1	1000	2	4	0	3.38×10^4	1.35
5	bpy	1	1000	2	4	0	4.36×10^4	1.46
6	PMDETA	1	500	2	2	0	5.80×10^3	1.08
7	PMDETA	1	500	2	2	0	7.90×10^3	1.09
8	PMDETA	1	500	2	2	0	1.43×10^4	1.09
9	PMDETA	1	1000	2	2	0	3.71×10^4	1.13
10	ME_6TREN	1	100	0.1	1	1	3.30×10^3	1.07
11	ME_6TREN	1	200	0.1	1	1	7.60×10^3	1.09
12	ME_6TREN	1	300	0.1	1	1	1.87×10^4	1.13
13	ME_6TREN	1	500	0.1	1	1	3.10×10^4	1.11
14	ME_6TREN	1	1000	0.1	1	1	4.50×10^4	1.13
15	ME_6TREN	1	1000	0.1	1	1	6.21×10^4	1.15

[a] The polymerization temperatures of entries 1−5, 6−9, and 10−15 are 110, 90, and 90 °C, respectively. [b] The polymerization of entries 1−9 and 10−15 was performed in bulk and in anisole (0.75 volume equiv vs monomer), respectively. [c] The number-average molar mass and molar mass distribution were determined by SEC on the basis of a conventional linear PSt calibration.

*Polystyrene [alkyne-(PSt-azide)$_2$] (**VI**).* A 100 mL round-bottom flask was charged with alkyne-(PSt-bromine)$_2$ (5.0 g, 0.66 mmol), DMF (30 mL), and NaN_3 (0.325 g, 5 mmol). The mixture was allowed to stir at room temperature for 36 h. After removing most of the solvent under reduced pressure, the remaining portion was diluted with CH_2Cl_2, and then precipitated into an excess of methanol. The sediments were redissolved in CH_2Cl_2 and passed through a neutral alumina column to remove residual sodium salts, and then precipitated into an excess of methanol. After it was dried in a vacuum oven overnight at room temperature, a linear seesaw-type polystyrene with one alkyne functional group and two azide functional groups was obtained.

*Defect-Free Hyperbranched PSt (**VII**).* The general procedure employed was as follows.[37] A three-necked flask equipped with a magnetic stirring bar and three rubber septum was charged with alkyne-(PSt-azide)$_2$ macromonomer (2 g, 0.263 mmol), PMDETA (109.5 μL, 0.526 mmol), and DMF (13.3 mL). The flask was degassed by four freeze−pump−thaw cycles, and then placed in a water bath thermostated at 35 °C. After ~2 min, CuBr (75 mg, 0.526 mmol) was introduced to start the polycondensation under N_2 flow. Samples were taken at timed intervals and precipitated into a mixture of methanol/water (90/10, v/v) and the products were washed with excess methanol. After drying in a vacuum oven overnight at 40 °C, the resultant hyperbranched polystyrene was analyzed by SEC and LLS.

Furthermore, the resultant hyperbranched polystyrene chains were fractionated by precipitation as follows. (1) The sample was dissolved in

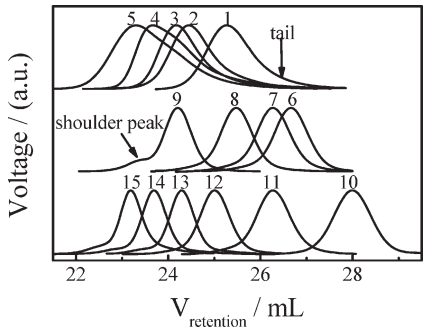

Figure 1. SEC curves of linear polystyrene macromonomers prepared via ATRP using bpy, PMDETA, ME_6TREN as ligand, respectively, and curves 1−5, 6−9, and 10−15 correspond to entries 1−5, 6−9, and 10−15 in Table 1.

toluene at room temperature with a concentration around 0.01 g/mL in a round-bottom flask; (2) methanol was slowly dropped in until the solution became milky; (3) the solution temperature controlled by a water bath (±0.1 °C) was slightly raised until the solution became clear again; (4) the solution was slowly cooled until it became slightly milky; and (5) the solution temperature was maintained to allow a very small fraction of longest chains to precipitate. Steps 2−5 were repeated to obtain a total of 10 fractions with different overall molar masses, ranging from 4.80×10^5 to 3.05×10^7 g/mol.

RESULTS AND DISCUSSION

Scheme 2 shows our strategy of synthesizing seesaw-type macromonomer B∼∼∼∼A∼∼∼∼B. In this study, both normal ATRP and ARGET ATRP were adopted. PBMP was used as an initiator due to its high efficiency.[47] The two terminal bromo functional groups were converted to two azide end groups via their reaction with NaN_3.[48]

Synthesis of Alkyne-(PSt-bromine)$_2$ Macromonomer via ATRP. It has been known that chains with some highly reactive end-groups are required to prepare well-defined polymer materials made of telechelic or block chains. In ATRP, side reactions induced by outer sphere electron-transfer (OSET) not only reduce the functionality of polymer chains but also limit the chain length attainable with some monomers.[49] Although much effort has been devoted to improving the end-group functionality of polymer chains synthesized by ATRP, the results reported in literature were inconsistent.[50−52] Datta et al.[51] found that poly(ethyl acrylate) made with bpy as a ligand contained more remaining bromine end-groups than that prepared with PMDETA. However, Matyjaszewski et al.[50,52] showed that a more reducing catalytic system, such as PMDETA and Me_6TREN, could increase the chain end-group functionality. Here we compared the ATRP by using bpy, PMDETA and Me_6TREN, respectively, as a ligand.

The polymerization conditions and results are summarized in Figure 1 and Table 1. All the results indicate that using CuBr−Me_6TREN−$Sn(EH)_2$ as a catalyst, the polymerization is better controlled. When bpy is used as a ligand, the reaction temperature should be relatively higher because the CuBr−bpy complex has a higher redox potential than the CuBr−PMDETA and Cu−Me_6TREN complexes.[53] The width of molar mass distribution rapidly increases as the macromonomers become longer. The SEC curves clearly show a long low-molar-mass tail; presumably due to the serious chain termination at the relatively higher reaction temperature. The CuBr−PMDETA system leads

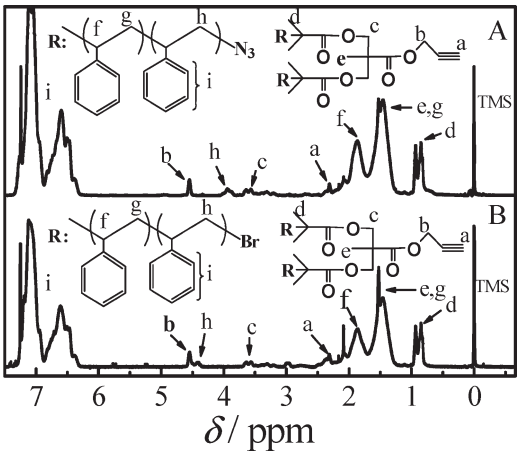

Figure 2. Comparison of ^{1}H NMR spectra of alkyne-(PSt-azide)$_2$ (A) and alkyne-(PSt-bromine)$_2$ (B, entry 10 in Table 1).

to a narrow molar mass distribution, slightly broadening as the chains are getting longer. There is a shoulder on the left of the SEC curve, marked by an arrow in Figure 1, when the average molar mass reaches $3-4 \times 10^4$ g/mol, presumably due to the increase of solution viscosity and some side reactions induced by CuBr.[50,54] The ARGET ATRP was carried out in anisole using Me_6TREN as a ligand and $Sn(EH)_2$ as a reductant, resulting in the longest macromonomers with the narrowest molar mass distribution. Our results reveal that lowering the CuBr concentration can effectively reduce side reactions. Hereafter, the linear macromonomer chains used are all prepared by the ARGET ATRP method.

Azidation of Linear PSt Macromonomers [alkyne-(PSt-bromine)$_2$]. Alkyne-(PSt-azide)$_2$ were prepared by an efficient substitution reaction of bromine in alkyne-(PSt-bromine)$_2$ with NaN_3 in DMF for 36 h.[48] Figure 2 shows a comparison of two ^{1}H NMR spectra of alkyne-(PSt-bromine)$_2$ and alkyne-(PSt-azide)$_2$. Besides the broad aromatic and aliphatic regions of styrene monomer and some signals from the initiator, two signals (H_h), originating from each end of the chain, are visible in their ^{1}H NMR spectra. The signal of the proton located at the chain end changes from 3.80 to 4.10 ppm (H_h in Figure 2B) to 4.30−4.50 ppm (H_h in Figure 2A), indicating a successful substitution. We estimated the average azide chain-end functionality (f) of the chains prepared by ARGET ATRP to be ∼99% from the area ratio of the H_h and H_b peaks in Figure 2A, i.e., f = functionality (%) = $100(H_h/H_b)$, which indicates that the loss of terminal bromine group is negligible and the azidation reaction was nearly complete, resulting in a set of narrowly distributed and highly functional linear seesaw-type macromonomer chains (azide∼∼∼∼alkyne∼∼∼∼azide) with different lengths.

Self-Polycondensation of Alkyne-(PSt-azide)$_2$ Macromonomer via "Click" Chemistry. As discussed before, using linear long B∼∼∼∼A∼∼∼∼B macromonomers, we are able to prepare large "defect-free" hyperbranched chains with uniform subchains, as shown in Scheme 2. Note that there still exists one inevitable and possible "defect" inside each resultant hyperbranched chain, i.e., the cyclization (self-looping) due to the intrachain coupling. As expected, the cyclization of each macromonomer itself in dilute solution is more serious but it can be reduced if the initial macromonomer concentration is high. However, the cyclization should not strongly affect the reaction

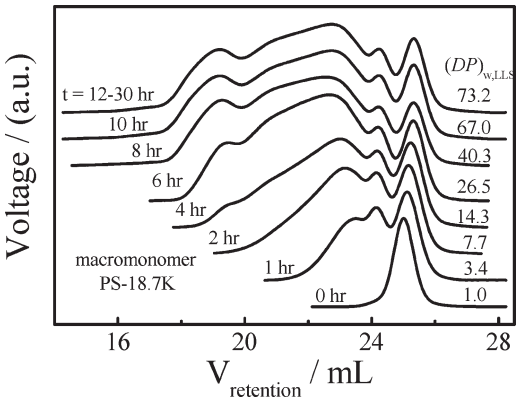

Figure 3. Reaction time dependent SEC curves of hyperbranched polystyrenes obtained from poly condensation of PS-18.7K, where C_0 = 0.15 g/mL.

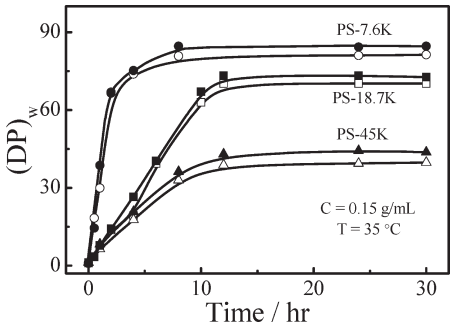

Figure 4. Macromonomer length dependent hyperbranched polystyrenes, where filled and hollow symbols represent results from stand-alone static LLS and SEC−MALLS, respectively.

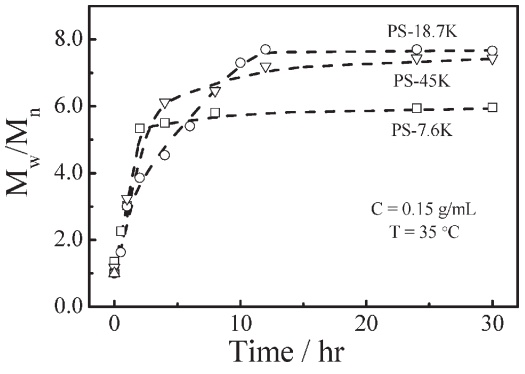

Figure 5. Reaction time dependent polydispersity index (M_w/M_n) of hyperbranched polystyrenes prepared with different initial macromonomers.

kinetics on the basis of our novel design. In order to obtain large hyperbranched chains, we need a highly efficient reaction between functional groups A and B without any side reactions. The alkyne−azide "click" cycloaddition used in the current study is the most suitable because of its high efficiency and low susceptibility to side reactions without oxygen.[55−57] DMF was used as solvent in the self-poly condensation of alkyne-(PSt-azide)$_2$ after the removal of oxygen at 35 °C with a catalyst of CuBr−PMDETA. We first investigated how the initial molar mass and concentration of alkyne-(PSt-azide)$_2$ affect the kinetics of the self-polycondensation of linear seesaw-type macromonomers.

Note that it is better to describe the self-polycondensation in terms of the average degree of polycondensation (DP), instead of the number and weight-average molar mass (M_n and M_w), because initial macromonomers have different lengths, where DP is defined as the number of macromonomers chemically coupled together inside each hyperbranched polystyrene chain; namely, $(DP)_n = M_{n,hyperbranched}/M_{n,macromonomer}$ and $(DP)_w = M_{w,hyperbranched}/M_{w,macromonomer}$. We prefer to use $(DP)_w$ to describe the polycondensation kinetics because it is the weight-average molar mass that was measured in SEC−RI or SEC−MALLS. As the reaction proceeds, M_w and $(DP)_w$ increase more rapidly than M_n and $(DP)_n$ (we will discuss this point later in Figure 4). Hereafter for the convenience of discussion, we rename entries 11, 12, and 14 in Table 1 as PS-7.6K, PS-18.7K and PS-45K to reflect their molar mass, respectively.

Effect of Macromonomer Length. Figure 3 shows SEC curves of hyperbranched polymers obtained from the self-polycondensation of PS-18.7K in DMF at 35 °C after different reaction times. As the reaction proceeds, the macromonomer peak becomes smaller and the large hyperbranched polymer peaks are emerging after a few hours, as shown by the shoulder with a retention volume less than 20 mL. However, there still exist about 10% macromonomers estimated from its peak area and the whole area of GPC trace. Figure 3 shows that the self-polycondensation reaction essentially stops after ~10 h, faster than what we expected. However, it is known that refractive index (RI) detector measures the polymer concentration, insensitive to the molar mass and chain size. Moreover, SEC−RI−PSt-calibration is not able to effectively distinguish polymer chains with a similar hydrodynamic volume but different topologic structures. Therefore, a large deviation from the true molar mass could occur in the high molar mass range, leading to a notable change in $(DP)_w$. To avoid such a problem, we further used a combination of SEC and MALLS as well as our stand-alone static LLS to characterize the absolute weight-average molar mass of each hyperbranched sample to obtain the true $(DP)_w$ and M_w/M_n. The results are summarized in Figures 4−7.

Figure 4 shows that large hyperbranched PSt chains are formed and their final average degree of self-polycondensation $(DP)_w$ increases from 40 to 81 as the initial molar mass of macromonomers decreases from 4.50×10^4 to 7.60×10^3 g/mol, presumably because of two following reasons. (1) The functional end groups on longer initial chains are much less reactive because they are wrapped inside individual coiled chains, and (2) the total concentration of the functional end groups is less for a given weight concentration (g/mL), also reflecting in its relatively lower reaction rate. Hutchings et al.[35,36] previously reported the preparation of hyperbranched polystyrenes with a moderate $(DP)_w$ (10−17) via the Williamson coupling reaction. Pan et al.[37] synthesized hyperbranched polystyrenes with a higher $(DP)_w$ (39−65) but much shorter Y-type macromonomers (~10^3 g/mol). It is worth noting that by increasing the initial macromonomer concentration, we are able to further increase $(DP)_w$, resulting in huge hyperbranched polystyrene chains but their characterization is rather difficult.

An attentive reader might notice that $(DP)_{w,LLS}$ is slightly higher than $(DP)_{w,MALLS}$ in the high molar mass range. Such a difference is attributed to few possible reasons. (1) In MALLS, 18 diodes, starting with the lowest angle of 22.5°, are less sensitive

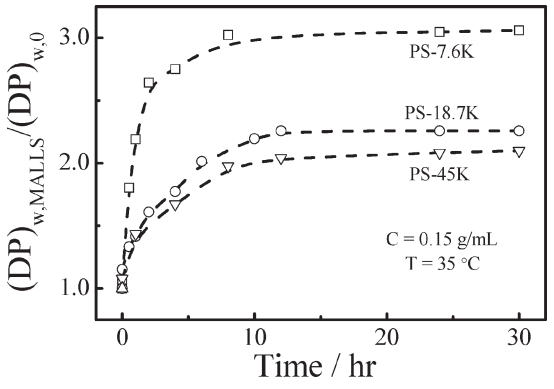

Figure 6. Reaction time dependence of $(DP)_{w,SEC\text{-}MALLS}/(DP)_{w,SEC\text{-}RI}$ of hyperbranched polystyrenes, where $(DP)_{w,SEC\text{-}MALLS}$ and $(DP)_{w,SEC\text{-}RI}$ were respectively measured using a combination of SEC with a RI and a MALLS detector.

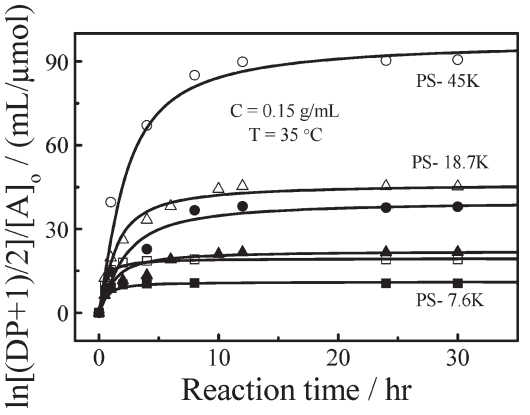

Figure 7. Reaction time dependent $\ln[(DP + 1)/2]/[A]_o$ for macromonomers with different lengths, where filled symbols, hollow symbols and lines, respectively, represent experimental $(DP)_n$, $(DP)_w$ and fitting curves using eq 7 with $k_{AB,0} = 1.2 \times 10^5$ and 2.8×10^5 mL/(mol·h) for $(DP)_n$ and $(DP)_w$, respectively.

with a high dark counters in comparison with the specially selected APD detector used in our stand-alone LLS, (2) for large hyperbranched chains, the condition of $q\langle R_g\rangle < 1$ is not maintainable with a sufficient number of angles in MALLS, and (3) the concentration of each fraction in SEC-MALLS is relatively lower so that the measured intensity of the scattered light is much weaker than that in our stand-alone LLS, especially in the lower and higher molar mass tails. Nevertheless, $(DP)_{w,MALLS}$ generally agrees well with $(DP)_{w,LLS}$, and the difference is less than ~7%.

Figure 5 shows that the polydispersity index (M_w/M_n) (determined by MALLS detector) increases with the reaction time, partially because of the slower increase of M_n (not shown). It is known that in the self-polycondensation of B~~~~A~~~~B, hyperbranched chains with more azide groups are ready to react with macromonomers but more difficult to react with each other because there is only one hiding A group inside each hyperbranched chain. However, the coupling between two hyperbranched chains in the later stage of reaction makes M_w to increase much fast than M_n. This is why M_w/M_n quickly rises to 5.8−7.7.

Figure 6 shows the ratio of $(DP)_{w,SEC\text{-}MALLS}/(DP)_{w,SEC\text{-}RI}$ of hyperbranched polystyrenes rapidly increases to 3.1 (PS-7.6K), 2.3 (PS-18.7K), and 2.1 (PS-45K), respectively, with the reaction time. The deviation of $(DP)_{w,SEC\text{-}MALLS}$ away from $(DP)_{w,SEC\text{-}RI}$ clearly shows that SEC with the conventional universal polystyrene calibration leads to a much underestimated molar mass for large hyperbranched chains. Therefore, it should be avoided in the study of branched chains because they have a much smaller hydrodynamic volume than their linear counterparts with a similar molar mass. In other words, $(DP)_{w,SEC\text{-}MALLS}/(DP)_{w,SEC\text{-}RI}$ reflects the hydrodynamic volume difference between hyperbranched and linear chains; namely, $(DP)_{w,SEC\text{-}MALLS}/(DP)_{w,SEC\text{-}RI}$ increases with the compactness of hyperbranched chains. For a meaningful comparison between hyperbranched and linear chains, we have to fractionate each resultant hyperbranched polystyrene sample to obtain narrowly distributed chains with uniform subchains but different overall molar masses. We will come back to this point later.

On the basis of Figure 4 and considering the nature of the self-polycondensation, we can assume that it follows the second-order kinetics, i.e.

$$-\mathrm{d[A]}/\mathrm{d}t = k_{AB}[A][B] \tag{3}$$

where [A] and [B] represent the molar concentrations of alkyne and azide groups, respectively; $[B]_o = 2[A]_o$ at $t = 0$; $[B] = [B]_o - ([A]_o - [A]) = [A]_o + [A]$ at $t = t$ so that eq 3 is rewritten as

$$-\mathrm{d[A]}/\mathrm{d}t = k_{AB}([A]_o + [A])[A] \tag{4}$$

where [A] can be replaced by DP because $DP = [A]_o/[A]$ by its definition. Finally, we have

$$\ln\frac{DP + 1}{2} = [A]_0\int_0^t k_{AB}\,\mathrm{d}t \tag{5}$$

It shows that at $t = 0$, DP = 1, and at $t \gg 1$, DP approaches an infinite if k_{AB} is a constant, i.e., resulting in one infinitely large hyperbranched polymer chain, which is chemically reasonable. However, our results reveal that the reaction slows down and DP approaches a constant when $t \gg 1$, presumably due to a decrease of the reactivity of the alkyne group inside each hyperbranched chain. At the initial stage, most of the alkyne groups are on linear macromonomers so that they can easily react with each other and with the azide groups on the periphery of a hyperbranched chain. As the reaction proceeds, the number of macromonomers decreases. When most of initial macromonomers are consumed, further polycondensation mostly involves the intrachain cyclization or the self-looping. It would be rather difficult for one alkyne group entrapped inside one hyperbranched chain to react with the azide groups on another chain. Note that the self-looping has no contribution to our experimentally measured values of DP. Considering such a physical nature, we assume that

$$k_{AB} = k_{AB,0}\frac{1}{1 + (\beta t)^2} \tag{6}$$

where $k_{AB,0}$ is the initial rate constant at $t = 0$ and β is a constant, so that eq 5 is rewritten as

$$\ln\frac{DP + 1}{2} = \frac{[A]_0 k_{AB,0}}{\beta}\arctan(\beta t) \tag{7}$$

It describes our experimental results well; namely, DP = 1 at $t = 0$, and $DP = k_{AB,0}\pi/(2\beta)$, at $t \gg 1$. In principle, we can obtain $[A]_o k_{AB,0}$ from the initial slope, $k_{AB,0}\pi/(2\beta)$ from the plateau value at $t \gg 1$, and β from a combination of $[A]_o k_{AB,0}$ and $k_{AB,0}\pi/(2\beta)$ since we know $[A]_0$.

Table 2. Calculated Values of β for Macromonomers with Different Initial Lengths

macromonomer	$[A]_o$, μmol/mL	β/h^{-1} from $(DP)_n$, $k_{AB,0} = 1.2 \times 10^5$ mL/(mol·h)	β/h^{-1} from $(DP)_w$, $k_{AB,0} = 2.8 \times 10^5$ mL/(mol·h)
PS-7.6K	19.7	1.71	2.25
PS-18.7K	8.00	0.85	0.95
PS-45K	3.33	0.47	0.45

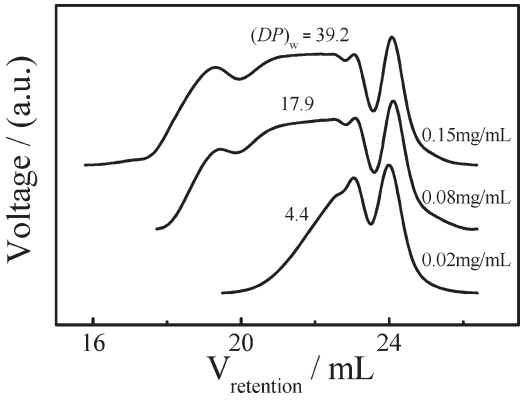

Figure 8. Initial macromonomer concentration dependence of SEC curves of resultant hyperbranched polystyrene samples after 48-h self-polycondensation of PS-45K at 35 °C.

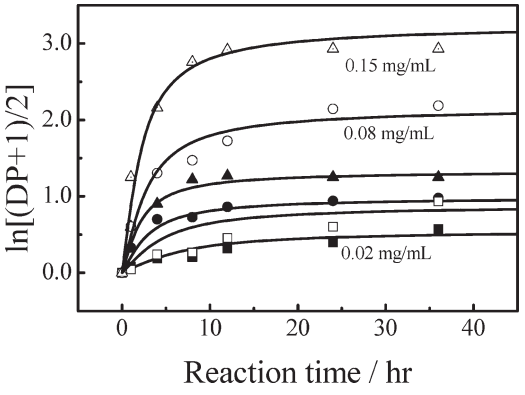

Figure 9. Reaction time dependence of $\ln[(DP + 1)/2]$ with different initial PS-45K concentrations, where filled and hollow symbols, and lines respectively represent experimental $(DP)_n$, $(DP)_w$ and fitting curves using eq 7, where the values of $k_{AB,0}$ are previously determined.

However, we are not able to practically determine the accurate initial slope ($[A]_o k_{AB,0}$) because of a limited number of data points. Physically, it is reasonable to assume that $k_{AB,0}$ should be much less dependent on the initial concentration and length of macromonomers because it only reflects the initial reaction rate between A and B. Therefore, we are able to first use the iteration to estimate the average value of $k_{AB,0}$ for three different macromonomers used and then fix it in the fitting of our experimental data with eq 7, as shown in Figure 7. In this way, β is the only adjustable parameter in the fitting. It is clear that eq 7 represents our experimental data well for both $(DP)_w$ and $(DP)_n$.

Table 2 summarizes the fitting results of β for different macromonomers when $(DP)_n$ and $(DP)_w$ are respectively used. β decreases as the macromonomer becomes longer. Note that physically, $1/\beta$ is the time at which k_{AB} decreases to 50% of its initial value. The decrease of β means that it takes a longer time for the reaction between A and B on longer macromonomer chains to slow down, which is physically reasonable because most of the reaction occurs between macromonomers and hyperbranched chains except at the very initial stage wherein linear azide∼∼∼∼alkyne∼∼∼∼azide macromonomers react with each other.

Effect of Initial Macromonomer Concentration. Figure 8 shows that the macromonomer peak nearly remains at the same position but its relative height decreases during the reaction, clearly indicating that there is no obvious self-cyclization of individual macromonomer chains even at a concentration as low as 0.02 mg/mL. Otherwise, the macromonomer peak would shift to the right, toward a slightly larger retention volume.

Figure 9 shows how the average degree of self-polycondensation (DP) obtained using a combination of SEC and LLS varies with the reaction time (t) when different initial macromonomer (PS-45K) concentrations are used. The lines in Figure 9 are calculated using eq 7. It shows that for a given ratio of [macromonomer]:[CuBr]:[PMDETA] = 1:2:2, both the initial reaction rate and final degree of the self-polycondensation increase with the initial macromonomer concentration, agreeing well with the prediction of eq 7. It is worth-noting that eq 7 also shows that both the initial rate and final degree of the self-polycondensation are related to β. On the other hand, Figure 7 and Table 2 show that β is related to the molar mass (length) of macromonomer used.

As mentioned before, $1/\beta$ reflects the time at which k_{AB} decreases to 50% of its initial value; namely, $k_{AB} = k_{AB,0}/2$ at $t = 1/\beta$, where $k_{AB,0}$ is a constant. Let us assume that the reaction rate is mainly controlled by diffusion, related to the interchain distance (L) and the translational diffusion coefficient (D). As expected, L increases as the initial macromonomer concentration (C_0) decreases, i.e., $L \sim C_0^{-1/3}$. Therefore, it should take a longer time for one macromonomer to react with another when C_0 decreases. On the other hand, it has been well-known that D is scaled to the molar mass of a polymer chain as $D \sim M^{-\alpha}$ with $\alpha = 0.5-0.6$, depending on the solvent quality. As discussed before, each hyperbranched chain contains no more than one alkyne group wrapped inside. Therefore, it is rather difficult for an azide group on one hyperbranched chain to react with the alkyne group hidden inside another hyperbranched chain. The reaction should mainly occur between macromonomers (in the very initial stage) and between one macromonomers and one hyperbranched chain.

Figure 10 shows two scalings: $1/\beta \sim [C]^{-0.35}$ and $\sim M_w^{0.90}$, where we have converted the weight concentration (C) in Figure 7 to the molar concentration ([C]) by $[C] = C/M_w$. It is also worth-noting that in Figure 4 we varied the molar mass of macromonomer but fixed its initial weight concentration (C). Therefore, we have to convert C to [C] and introduce an additional $M_w^{-0.35}$ into the scaling; namely, the exponent (0.90) on M_w should be reduced to 0.55. A combination of both the [C] and M_w dependence of $1/\beta$ finally leads to $1/\beta \sim [C]^{-0.35} M_w^{0.55}$, indicating that $1/\beta$ is related to both the interchain distance and diffusion.

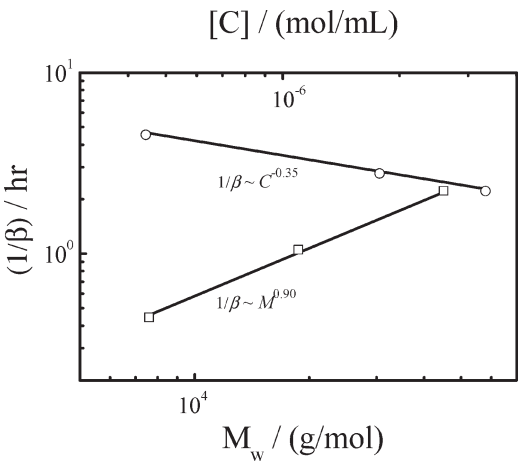

Figure 10. Macromonomer's molar concentration ([C]) and weight-average molar mass (M_w) dependence of $1/\beta$ obtained from reaction time dependence of $(DP)_w$ in Figures 7 and 9.

LLS Characterization of Fractionated Hyperbranched Chains. Figure 11 shows a typical Zimm plot of one narrowly distributed hyperbranched polystyrene fraction (Fraction 3 in Table 3). On the basis of eq 2, we are able to obtain the values of the weight-average molar mass (M_w), the average radius of gyration ($\langle R_g \rangle$) and the second virial coefficient (A_2) from the intercept and two slopes, respectively. The results together with the average hydrodynamic radius ($\langle R_h \rangle$) from dynamic LLS are summarized in Table 3, where PS-18.7K was used.

Table 3 shows that the fractional precipitation method has successfully led to 10 relatively narrowly distributed hyperbranched polystyrene samples with $M_w/M_n < 1.3$ and over a wide range of molar mass. It is known that for hard spheres, hyperbranched chains and coiled linear chains, $\langle R_g \rangle/\langle R_h \rangle$ are 0.774, 1.0−1.4, and 1.5−1.8, respectively, depending on their distributions and solvent quality.[58−60] For these fractionated hyperbranched polystyrenes, $\langle R_g \rangle/\langle R_h \rangle$ varies between 1.2 and 1.4, as shown in Table 3, indicating that they are swollen in toluene (a very good solvent) with a relatively loose structure. Also note that smaller chains have a higher value of $\langle R_g \rangle/\langle R_h \rangle$, revealing that they have an even more open and lose chain conformation.

The difference between linear and branched chains become more obvious when the scattering factor $P(qR_g)$ versus qR_g is plotted,[62,63] as shown in Figure 12. Note that both $P(qR_g)$ and qR_g are dimensionless so that such a plot should be universal for a given type of chain topology. Indeed, the scattering factors of different fractions collapse into a master curve in the qR_g range studied, indicating that all the fractions are self-similar and following a similar scaling law at $qR_g > 1.5$. The negative slope represents the ensemble fractal dimension (d_f) that is close to the prediction for the reaction-limited cluster−cluster aggregation.[62,63]

The effect of branching is even better displayed in the Kratky plot; namely, $(qR_g)^2P(qR_g)$ versus qR_g, as shown in Figure 13. Theoretically, Burchard[62,63] deduced the scattering factor for AB_2-type hyperbranched chains as

$$p(qR_g) = \frac{1 + \frac{(qR_g)^2}{3n_B}}{\left[1 + \left(\frac{1 + n_B}{6n_B}\right)(qR_g)^2\right]^2} \quad (8)$$

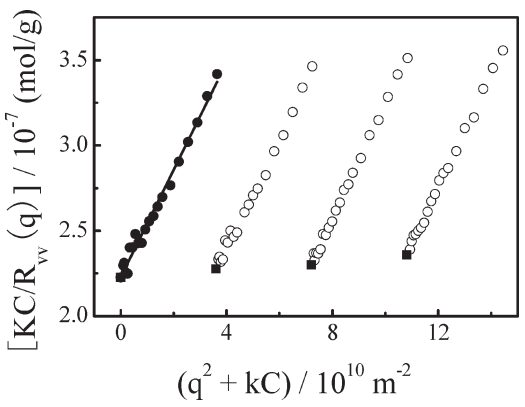

Figure 11. Typical Zimm plot of one hyperbranched polystyrene fraction in toluene at 25 °C, where C ranges from 5.0×10^{-5} to 1.5×10^{-4} g/mL.

Table 3. LLS Characterization of Hyperbranched Polystyrene Fractions in Toluene at 25 °C

fraction	M_w/(g/mol)	$\langle R_g \rangle$/nm	$\langle R_h \rangle$/nm[a]	$\langle R_g \rangle/\langle R_h \rangle$	M_w/M_n[b]	g[c]
1	3.05×10^7	173	140	1.2	1.35	0.25
2	1.09×10^7	99	78	1.3	1.24	0.28
3	4.50×10^6	67	51	1.3	1.20	0.37
4	2.68×10^6	52	40	1.3	1.25	0.40
5	1.85×10^6	44	35	1.3	1.10	0.47
6	1.61×10^6	41	31	1.3	1.13	0.47
7	1.21×10^6	36	28	1.3	1.16	0.52
8	8.70×10^5	32	24	1.3	1.12	0.61
9	6.20×10^5	28	20	1.4	1.08	0.66
10	4.80×10^5	24	18	1.4	1.11	0.70

[a] Dynamic LLS was carried out at a fixed low angle of 12°. [b] M_w/M_n was estimated from relative line-width (μ_2) of diffusion coefficient distribution and average diffusion coefficient ($\langle D \rangle$) by using $(1 + 4\mu_2/\langle D \rangle^2)$. [c] $g = \langle R_g^2 \rangle_{branch}/\langle R_g^2 \rangle_{linear}$ and $\langle R_g \rangle_{linear}$ (nm) = $1.23 \times 10^{-2} M_w^{0.594\,61}$.

where n_B is the number of branching points per hyperbranched chain and expressed as

$$n_B = \frac{(\phi + \varphi) - (\phi^2 + \varphi^2)}{(\phi^2 + \varphi^2)[1 - (\phi + \varphi)]} \quad (9)$$

where ϕ in our case is the probability of group A in one macromonomer (B∼∼∼∼A∼∼∼∼B) reacted with the first group B in another macromonomer; and φ is the probability of group A reacted with the second group B. Experimentally, we found that $n_B \simeq 13.2$, as shown in Figure 13, where we also plot two limiting cases: $n_B = \infty$ (hard sphere) and 1 (linear chains). It is clear that our hyperbranched chains are less draining and close to a hard sphere. In principle, $\phi = 0.5$ because the two unreacted A groups on a macromonomer should have an equal probability to react the A group on another macromonomer. Using our fitting result of value of $n_B = 13.2$, we could numerically calculate $\varphi = 0.42$ on the basis of eq 9, smaller than 0.5, as expected, because the steric effect makes the second B group less reactive. It is worth-noting that in our simple discussion, the effect of excluded volume is neglected.[63,64]

^{1}H NMR is often used to estimate the degree of branching (DB) of hyperbranched chains made of small multifunctional

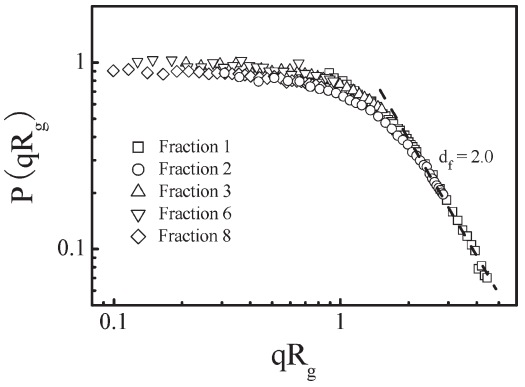

Figure 12. qR_g-dependence of scattering factor $P(qR_g)$ of different fractions of hyperbranched polystyrenes synthesized using PS-18.7K.

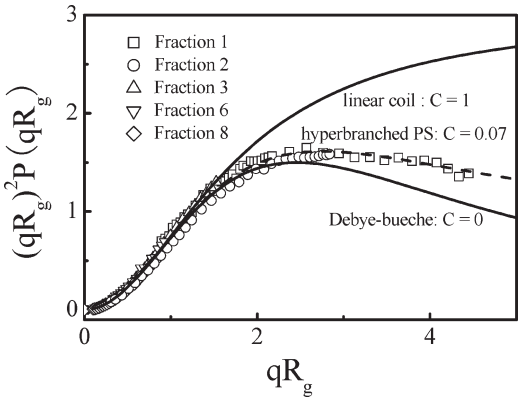

Figure 13. Kratky plots for hyperbranched polystyrenes synthesized using PS-18.7K, where $C = 1/n_B$, two solid lines represent fitting curves for linear coiled chains and Debye-bueche hard spheres, respectively.

monomers.[34,40] However, it becomes much less effective for hyperbranched chains prepared from large macromonomers because of a limited branching points in comparison with a large number of other chemical groups. As discussed before, large hyperbranched chains have a smaller root-mean-square gyration radius $\langle R_g \rangle$ and a lower intrinsic viscosity ($[\eta]$) than their corresponding linear counterparts with a similar molar mass.[31,43,65,66] The ratio of the mean-square radii of gyration of a hyperbranched chain and a linear chain with an identical molar mass ($\langle R_g^2 \rangle_{branch}$ and $\langle R_g^2 \rangle_{linear}$), known as the contraction factor (g), is another way to describe the degree of branching (DB).

Lubensky et al.[67] used the Flory's approximation to find that in an athermal solvent, the root-mean-square radius of gyration (R_g) is scaled to the overall degree of polymerization of ideal branched chains (N) with a scaling exponent (ν) of 0.5. Further, Render[68] found that for ideal branched chains, ν is in the range 0.43−0.53 in the Monte Carlo simulation, covering the Lubensky's prediction. Note that these previous studies were mostly based on an assumption of ideal branched chains; namely, with uniform subchains between two neighboring branching points. To the best of our knowledge, there have been few reported experimental studies on conformational properties of hyperbranched polymers with long subchains but no study on truly ideal or "defect-free" hyperbranched chains.

Armed with such 10 relatively narrowly distributed hyperbranched polystyrene fractions with uniform subchains over a wide molar mass range, we are in a much better position to determine the scaling law between the chain size and molar mass of ideal branched chains. Figure 14 shows how the average root-mean square radius of gyration $\langle R_g \rangle$ and the average hydrodynamic radius $\langle R_h \rangle$ depend on the weight-average molar mass (M_w) of "defect-free" hyperbranched chains. The lines represent $\langle R_g \rangle$ (nm) = 5.53 × 10^{-2} $M_w^{0.464}$ and $\langle R_h \rangle$ (nm) = 2.95 × 10^{-2} $M_w^{0.489}$, which agrees well with previous predictions.[67,68] Further, Figure 15 shows that in toluene at 25 °C, the contraction factor (g) is scaled to M_w as $g = 2.02 \times 10^1 M_w^{-0.260}$.

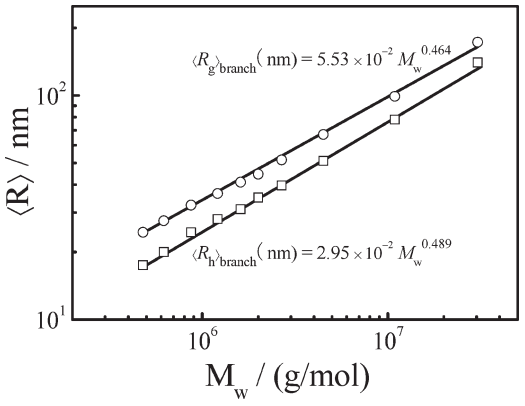

Figure 14. Weight average molar mass (M_w) dependence of average gyration and hydrodynamic radii ($\langle R_g \rangle$ and $\langle R_h \rangle$) in toluene at 25 °C, where 10 fractions were obtained from hyperbranched chains synthesized using PS-18.7K.

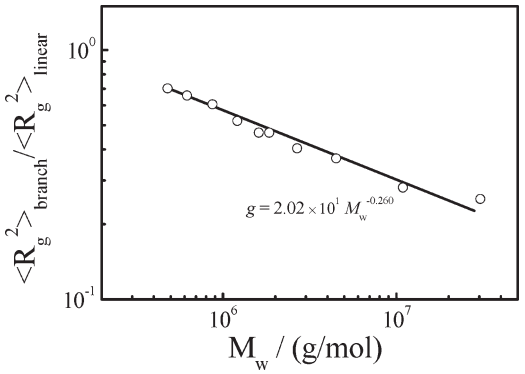

Figure 15. Weight-average molar mass (M_w) dependence of contraction factor ($g = \langle R_g^2 \rangle_{branch}/\langle R_g^2 \rangle_{linear}$) in toluene at 25 °C, where 10 fractions were from hyperbranched chains synthesized using PS-18.7K.

CONCLUSION

In conclusion, we have successfully prepared "defect-free" hyperbranched polystyrene chains with uniform subchains by using seesaw-type macromonomers [azide∼∼∼∼alkyne∼∼∼∼azide], where ∼∼∼∼ is polystyrene chain with a controllable length and two reactive functional groups (alkyne and azide) can be "clicked" together. The chain length between two functional groups can be precisely adjusted by atom transfer radical polymerization (ATRP). Our results confirmed that each of the two ends of the macromonomer chain can be effectively functionalized with a reactive bromo group by using the activators regenerated by electron transfer for atom transfer radical polymerization (ARGET ATRP) method with propargyl 2,2-bis((2′-bromo-2′-methylpropanoyloxy)methyl)propionate as an initiator. The

reaction rate of the self-polycondensation of alkyne-(PSt-azide)$_2$ increases with the initial concentration of macromonomers but is less influenced by the mocromonomer's length. The kinetics is the second order but with a time-dependent rate constant: $k_{AB} = k_{AB,0}/[1 + (\beta t)^2]$, where $k_{AB,0}$ is the rate constant at $t = 0$ and $1/\beta$ is a time at which k_{AB} becomes half of $k_{AB,0}$. Our results reveal that $1/\beta$ is scaled to the macromonomer's molar concentration ([C]) and molar mass (M) as $1/\beta \sim [C]^{-0.35} M^{0.55}$, indicating that $1/\beta$ is governed by the interchain distance and diffusion, simultaneously. A combination of static and dynamic LLS characterization of 10 relatively narrowly distributed hyperbranched polystyrene fractions, prepared by the gradual precipitation method, reveals that the hyperbranched chains have (1) an open and loose structure due to long subchains, (2) a fractal dimension of $d_f \simeq 2$, indicating that they are formed by the reaction-limited cluster−cluster aggregation mechanism, and (3) a hyperbranching parameter of $n_B = 13.2$, revealing that the chains are more in resemblance to a spherical structure, and (4) the chain sizes are scaled to the weight-average molar mass (M_w) as $\langle R_g \rangle \sim M_w^{0.464}$ and $\langle R_h \rangle \sim M_w^{0.489}$ in toluene at 25 °C, agreeing well with previous predictions in literature; Using seesaw-type B∼∼∼∼A∼∼∼∼B macromonomers, we have developed a very powerful and convenient approach to prepare large "defect-free" hyperbranched polymer chains for their subsequent structure−property studies.

AUTHOR INFORMATION

Corresponding Author

*E-mail: (C.W.) chiwu@cuhk.edu.hk; (W.H.) wdhe@ustc.edu.cn.

ACKNOWLEDGMENT

The financial support of the National Natural Scientific Foundation of China Projects (51173177 and 20934005) and the Hong Kong Special Administration Region Earmarked Projects (CUHK4046/08P, 2160365; CUHK4039/08P, 2160361; and CUHK4042/09P, 2160396) is gratefully acknowledged.

REFERENCES

(1) Cao, Q.; Liu, P. *J. Mater. Sci.* **2007**, *42*, 5661.
(2) Chen, Y.; Shen, Z.; Pastor-Pérez, L.; Frey, H.; Stiriba, S. E. *Macromolecules* **2004**, *38*, 227.
(3) Hawker, C. J.; Chu, F.; Pomery, P. J.; Hill, D. J. T. *Macromolecules* **1996**, *29*, 3831.
(4) Liu, C.; Gao, C.; Yan, D. *Macromolecules* **2006**, *39*, 8102.
(5) Yang, Y.; Xie, X.; Yang, Z.; Wang, X.; Cui, W.; Yang, J.; Mai, Y. W. *Macromolecules* **2007**, *40*, 5858.
(6) Schulz, M.; Tanner, S.; Barqawi, H.; Binder, W. H. *J. Polym. Sci., Part A: Polym.Chem.* **2010**, *48*, 671.
(7) Xu, J.; Ye, J.; Liu, S. *Macromolecules* **2007**, *40*, 9103.
(8) Lonsdale, D. E.; Monteiro, M. J. *Chem. Commun.* **2010**, *46*, 7945.
(9) Furukawa, T.; Ishizu, K. *Macromolecules* **2005**, *38*, 2911.
(10) Okumoto, M.; Nakamura, Y.; Norisuye, T.; Teramoto, A. *Macromolecules* **1998**, *31*, 1615.
(11) Babin, J.; Taton, D.; Brinkmann, M.; Lecommandoux, S. *Macromolecules* **2008**, *41*, 1384.
(12) Ishizu, K.; Furuta, Y.; Okamoto, N.; Uchida, S.; Ozawa, M. *Macromol. Chem. Phys.* **2010**, *211*, 1984.
(13) Gungor, E.; Durmaz, H.; Hizal, G.; Tunca, U. *J. Polym. Sci., Part A: Polym.Chem.* **2008**, *46*, 4459.
(14) Clarke, N.; Luca, E. D.; Dodds, J. M.; Kimani, S. M.; Hutchings, L. R. *Eur. Polym. J.* **2008**, *44*, 665.
(15) Hutchings, L. R. *Soft Matter* **2008**, *4*, 2150.
(16) Wang, W. J.; Wang, D.; Li, B. G.; Zhu, S. *Macromolecules* **2010**, *43*, 4062.
(17) Peleshanko, S.; Gunawidjaja, R.; Petrash, S.; Tsukruk, V. V. *Macromolecules* **2006**, *39*, 4756.
(18) Hawker, C. J.; Frechet, J. M. J.; Grubbs, R. B.; Dao, J. *J. Am. Chem. Soc.* **1995**, *117*, 10763.
(19) Fréchet, J. M. J.; Henmi, M.; Gitsov, I.; Aoshima, S.; Leduc, M. R.; Grubbs, R. B. *Science* **1995**, *269*, 1080.
(20) Liu, M.; Vladimirov, N.; Fréchet, J. M. J. *Macromolecules* **1999**, *32*, 6881.
(21) Magnusson, H.; Malmström, E.; Hult, A. *Macromol. Rapid Commun.* **1999**, *20*, 453.
(22) Emrick, T.; Chang, H. T.; Fréchet, J. M. J. *Macromolecules* **1999**, *32*, 6380.
(23) Kong, J.; Schmalz, T.; Motz, G. N.; Müller, A. H. E. *Macromolecules* **2011**, *44*, 1280.
(24) Oguz, C.; Unal, S.; Long, T. E.; Gallivan, M. A. *Macromolecules* **2007**, *40*, 6529.
(25) Vanjinathan, M.; Shanavas, A.; Raghavan, A.; Nasar, A. S. *J. Polym. Sci., Part A: Polym.Chem.* **2007**, *45*, 3877.
(26) Zhu, Z.; Pan, C. *Macromol. Chem. Phys.* **2007**, *208*, 1274.
(27) Li, J.; Sun, M.; Bo, Z. *J. Polym. Sci., Part A: Polym.Chem.* **2007**, *45*, 1084.
(28) Ghosh, A.; Banerjee, S.; Komber, H.; Lederer, A.; Häussler, L.; Voit, B. *Macromolecules* **2010**, *43*, 2846.
(29) Adam, M.; Delsanti, M.; Munch, J. P.; Durand, D. *J. Phys. Paris* **1987**, *48*, 1809.
(30) de Gennes, P. G. *Biopolymers.* **1968**, *6*, 715.
(31) Zimm, B. H.; Stockmayer, W. H. *J. Chem. Phys.* **1949**, *17*, 1301.
(32) Unal, S.; Yilgor, I.; Yilgor, E.; Sheth, J. P.; Wilkes, G. L.; Long, T. E. *Macromolecules* **2004**, *37*, 7081.
(33) Unal, S.; Ozturk, G.; Sisson, K.; Long, T. E. *J. Polym. Sci., Part A: Polym.Chem.* **2008**, *46*, 6285.
(34) Trollsas, M.; Kelly, M. A.; Claesson, H.; Siemens, R.; Hedrick, J. L. *Macromolecules* **1999**, *32*, 4917.
(35) Hutchings, L. R.; Dodds, J. M.; Roberts-Bleming, S. J. *Macromolecules* **2005**, *38*, 5970.
(36) Hutchings, L. R.; Dodds, J. M.; Roberts-Bleming, S. J. *Macromol. Symp.* **2006**, *240*, 56.
(37) Kong, L. Z.; Sun, M.; Qiao, H. M.; Pan, C. Y. *J. Polym. Sci., Part A: Polym.Chem.* **2010**, *48*, 454.
(38) Konkolewicz, D.; Gray-Weale, A.; Perrier, S. b. *J. Am. Chem. Soc.* **2009**, *131*, 18075.
(39) Trollsås, M.; Hedrick, J. L. *Macromolecules* **1998**, *31*, 4390.
(40) Choi, J.; Kwak, S. Y. *Macromolecules* **2003**, *36*, 8630.
(41) He, C.; Li, L. W.; He, W. D.; Jiang, W. X.; Wu, C. *Macromolecules* **2011**, *44*, 6233.
(42) Queffelec, J.; Gaynor, S. G.; Matyjaszewski, K. *Macromolecules* **2000**, *33*, 8629.
(43) Zimm, B. H. *J. Chem. Phys.* **1948**, *16*, 1099.
(44) Chu, B. *Laser Scattering*, 2nd ed.; Academic Press: New York, 1991.
(45) Wu, C.; Xia, K. Q. *Rev. Sci. Instrum.* **1994**, *65*, 587.
(46) Berne, B.; Pecroa, R. *Dynamic Light Scattering*; Plenum Press: New York, 1976.
(47) Liu, Q.; Zhao, P.; Chen, Y. *J. Polym. Sci., Part A: Polym.Chem.* **2007**, *45*, 3330.
(48) Laurent, B. A.; Grayson, S. M. *J. Am. Chem. Soc.* **2006**, *128*, 4238.
(49) Tsarevsky, N. V.; Braunecker, W. A.; Matyjaszewski, K. *J. Organomet. Chem.* **2007**, *692*, 3212.
(50) Lutz, J. F.; Matyjaszewski, K. *J. Polym. Sci., Part A: Polym.Chem.* **2005**, *43*, 897.
(51) Datta, H.; Bhowmick, A. K.; Singha, N. K. *J. Polym. Sci., Part A: Polym.Chem.* **2007**, *45*, 1661.
(52) Jakubowski, W.; Kirci-Denizli, B.; Gil, R. R.; Matyjaszewski, K. *Macromol. Chem. Phys.* **2008**, *209*, 32.
(53) Xia, J.; Matyjaszewski, K. *Macromolecules* **1997**, *30*, 7697.

(54) Matyjaszewski, K.; Davis, K.; Patten, T. E.; Wei, M. *Tetrahedron* **1997**, *53*, 15321.
(55) Binder, W. H.; Sachsenhofer, R. *Macromol. Rapid Commun.* **2007**, *28*, 15.
(56) Binder, W. H.; Sachsenhofer, R. *Macromol. Rapid Commun.* **2008**, *29*, 952.
(57) Bock, V. D.; Hiemstra, H.; van Maarseveen, J. H. *Eur. J. Org. Chem.* **2006**, 51.
(58) Burchard, W.; Schmidt, M.; Stockmayer, W. H. *Macromolecules* **1980**, *13*, 1265.
(59) Vagberg, L. J. M.; Cogan, K. A.; Gast, A. P. *Macromolecules* **1991**, *24*, 1670.
(60) Peng, S. F.; Wu, C. *Macromolecules* **1999**, *32*, 585.
(61) Teraoka, I. *Polymer Solution*; John Wiley & Sons, Inc: New York, 2002.
(62) Burchard, W. *Macromolecules* **1977**, *10*, 919.
(63) Burchard, W. *Adv. Polym. Sci.* **1983**, *48*, 1.
(64) Burchard, W. *Macromolecules* **2004**, *37*, 3841.
(65) Voit, B. I.; Lederer, A. *Chem. Rev.* **2009**, *109*, 5924.
(66) Gao, C.; Yan, D. *Prog. Polym. Sci.* **2004**, *29*, 183.
(67) Isaacson, J.; Lubensky, T. C. *J. Phys., Lett.* **1980**, *41*, 469.
(68) Render, S. *J. Phys. A: Math. Gen* **1979**, *12*, L239.